doi:10.1016/j.jmb.2004.09.003 J. Mol. Biol. (2004) 343, 1055–1065

JMB

Available online at www.sciencedirect.com

SCIENCE DIRECT®

ELSEVIER

# Structure of a Human A-type Potassium Channel Interacting Protein DPPX, a Member of the Dipeptidyl Aminopeptidase Family

**Pavel Strop[1], Alexander J. Bankovich[2], Kirk C. Hansen[3] K. Christopher Garcia[2] and Axel T. Brunger[1]***

[1]*Howard Hughes Medical Institute and Departments of Molecular and Cellular Physiology, Neurology and Neurological Sciences, and Stanford Synchrotron Radiation Laboratory, Stanford University James H. Clark Center E300 318 Campus Drive, Stanford CA 94305, USA*

[2]*Department of Microbiology and Immunology, Stanford University School of Medicine Fairchild D319, 299 Campus Drive, Stanford, CA 94305-5124 USA*

[3]*Department of Pharmaceutical Chemistry, University of California San Francisco San Francisco, CA, 94143-0446 USA*

**Corresponding author*

It has recently been reported that dipeptidyl aminopeptidase X (DPPX) interacts with the voltage-gated potassium channel Kv4 and that co-expression of DPPX together with Kv4 pore forming α-subunits, and potassium channel interacting proteins (KChIPs), reconstitutes properties of native A-type potassium channels *in vitro*. Here we report the X-ray crystal structure of the extracellular domain of human DPPX determined at 3.0 Å resolution. This structure reveals the potential for a surface electrostatic change based on the protonation state of histidine. Subtle changes in extracellular pH might modulate the interaction of DPPX with Kv4.2 and possibly with other proteins. We propose models of DPPX interaction with the voltage-gated potassium channel complex. The dimeric structure of DPPX is highly homologous to the related protein DPP-IV. Comparison of the active sites of DPPX and DPP-IV reveals loss of the catalytic serine residue but the presence of an additional serine near the "active" site. However, the arrangement of residues is inconsistent with that of canonical serine proteases and DPPX is unlikely to function as a protease (dipeptidyl aminopeptidase).



*Keywords:* DPPX; DPP6; voltage gated potassium channel; dipeptidyl aminopeptidase; serine protease

## Introduction

Dipeptidyl aminopeptidase X (DPPX, also termed DPP6, BSPL, or potassium channel accelerating factor (KAF)) is a type II transmembrane protein belonging to the prolyl oligopeptidase family of serine proteases.[1–3] This family includes proteins such as DPP-IV[4] (CD26), fibroblast activation protein (FAP),[5] prolyl oligopeptidase (POP),[6] DPP8,[7] DPP9, and DPP10 (DPPY)[8] (K. Takimoto, personal communication). Prolyl oligopeptidases remove dipeptides from regulatory proteins and peptides.[9,10] DPP-IV, for example, plays an important role in regulation of physiological processes that include immune, metabolic, inflammatory, and central nervous system functions[11,12] by cleaving Xaa-Pro or Xaa-Ala from the N terminus of chemokines and neuropeptides. DPP-IV inactivates a variety of bioactive peptides including glucagon hormones such as GLP-1, which stimulate insulin secretion. Therefore, DPP-IV is a potential therapeutic target for treating type 2 diabetes.

Both DPPX and DPPY proteins have a substitution at the catalytic serine (aspartic acid in DPPX and glycine in DPPY) which appears to render them inactive proteases.[8,13] Mutagenesis of the aspartic acid residue in the active site back to serine in DPPX shows a twofold increase of protease activity compared to the wild-type DPPX. However, this DPPX variant engineered with a functional catalytic

Abbreviations used: DPPX, dipeptidyl aminopeptidase X; KChIP, potassium channel interacting protein; NCS, non-crystallographic symmetry; r.m.s.d., root-mean-square deviation; IEF, isoelectric focusing.

E-mail address of the corresponding author: brunger@stanford.edu

triad still has a 100-fold lower activity than wild-type DPP-IV.[1,13] These data indicate that DPPX lacks the traditional proteolytic activity of the other family members and that additional residues in the active site, apart from the catalytic triad, are important for DPP-IV like activity.[13]

In the absence of a known proteolytic role, DPPX has been identified as an associated component of an A-type $K^+$ channel.[3] The voltage-gated potassium channel family (Kv) is a class of ion channels that play important roles in regulating the excitability of electrically active cells.[14] The diversity of voltage-gated potassium channels is a result of both a large number of Kv subunits, as well as interactions of Kv pore forming α-subunits with auxiliary proteins.[15,16]

The Kv4 family of voltage-gated potassium channels is responsible for rapidly inactivating currents in the heart ($I_{TO}$) and in neurons ($I_{SA}$).[17] In the heart, Kv4 channels are responsible for initial re-polarization of the cardiac action potential.[18,19] In neurons, Kv4 channels regulate the propagation of action potential and the firing frequency.[20] In dopaminergic neurons, firing frequency modulates dopamine release and alterations in firing frequencies can induce Parkinsonian symptoms.[21] Kv4 channels therefore provide therapeutic targets for diseases such as Parkinson's and schizophrenia.[22] At present, Kv4 subunits are known to interact with potassium channel interacting proteins (KChIPs) and with DPPX/Y[3,23] (K. Takimoto, personal communication). KChIPs are calcium-sensing proteins that increase the current amplitude and alter Kv4 channel gating.[15,24–26] DPPX associates with Kv4 channels, facilitates Kv4 α-subunits trafficking to the membrane, and increases the rate of inactivation.[3,23] DPPY was also found to modulate Kv4 channel properties in a similar, but not identical fashion to DPPX[27] (K. Takimoto, personal communication). DPPY also immunoprecipates with Kv4 subunits, increases Kv4 current density, and alters Kv4 channel gating characteristics[27] (K. Takimoto, personal communication). Co-expression of DPPX, Kv4 pore forming α-subunits, and KChIPs, reconstitutes properties of native A-type potassium channels *in vitro*.[3]

The binding site of DPPX on the Kv4 channel is unknown at present. DPPX contains a very short intracellular tail (31–95 residues depending on the isoform), one putative transmembrane helix, and a large 749 amino acid extracellular domain. The interaction between DPPX and Kv4 is most likely mediated through the transmembrane helix and the extracellular domain. Here we present the structure of the extracellular domain of DPPX determined at 3.0 Å resolution. Comparison of the active sites of DPPX and DPP-IV explains why DPPX is unable to function as a dipeptidyl aminopeptidase. Based on the structure of DPPX and structural and biochemical data for potassium channel interacting proteins, we propose models of DPPX interactions with Kv4 α-subunits.

## Results

### Overall structure

DPPX exists as several splicing variants termed DPPX-L, DPPX-S, DPPX-N, and DPPX-O (K. Takimoto, personal communication). Here, we have chosen to use the numbering of the largest variant (DPPX-L). In this variant, the intracellular N terminus (residues 1–95) is followed by a putative transmembrane helix (residues 96–116) and a large extracellular domain (residues 116–865). The extracellular domain crystallized in space group $P2_1$ with two dimers in the asymmetric unit. The structure was determined by molecular replacement using DPP-IV[12] as a search model, which has 32% sequence identity and whose structure was previously determined at 2.5 Å. Six N-glycosylation sites were found in the DPPX structure with visible electron density for at least two *N*-acetyl-glucosamine moieties. The first ten and last 16 residues of the extracellular domain of DPPX were disordered. The final structure consists of 722 residues (127–849) of the extracellular domain. Data, refinement, and model statistics are shown in Table 1.

The structure of DPPX closely resembles that of the related DPP-IV.[12,28–30] Two monomers associate to form a homodimer (Figure 1(a)). Each monomer consists of an eight-bladed β-propeller domain (residues 142–322, and 351–581) (Figure 1(b)) and an α/β hydrolase domain (residues 127–142, and 581–849) (Figure 1(c)). Both the α/β hydrolase domain and the β-propeller domain participate in the formation of the dimer, generating a buried surface area of 2574 $Å^2$ (9% of the total surface area of a DPPX monomer). The dimer interface is formed by the last β-strand and the last two helices in the α/β hydrolase domain and by the β-hairpin insertion motif from the β-propeller domain (Figure 1). In

**Table 1.** Refinement and model statistics

| | |
|---|---|
| Space group | $P2_1$ |
| Cell dimensions | |
| *a*, *b*, *c* (Å) | 69.0, 170.2, 159.3 |
| β (°) | 92.1 |
| Resolution (Å) | 18.0–3.0 |
| Measured reflections | 288,512 |
| Unique reflections | 66,451 |
| $R_{merge}$ | 9.8 (37.4) |
| Completeness (%) | 90.6 (63.3) |
| $I/\sigma(I)$ | 15 (1.95) |
| Number of: protein atoms | 23,348 |
| Carbohydrate atoms | 825 |
| Water molecules | 51 |
| Overall *B*-factor value ($Å^2$) | 75.1 |
| $R_{cryst}$ (%) | 24.8 |
| $R_{free}$ (%) | 28.0 |
| Root-mean-square deviation | |
| Bonds | 0.007 |
| Angles | 1.50 |
| Ramachandran | |
| Most favored regions | 72.5 |
| Additional allowed regions | 24.0 |
| Generously allowed regions | 3.5 |
| Disallowed regions | 0.0 |

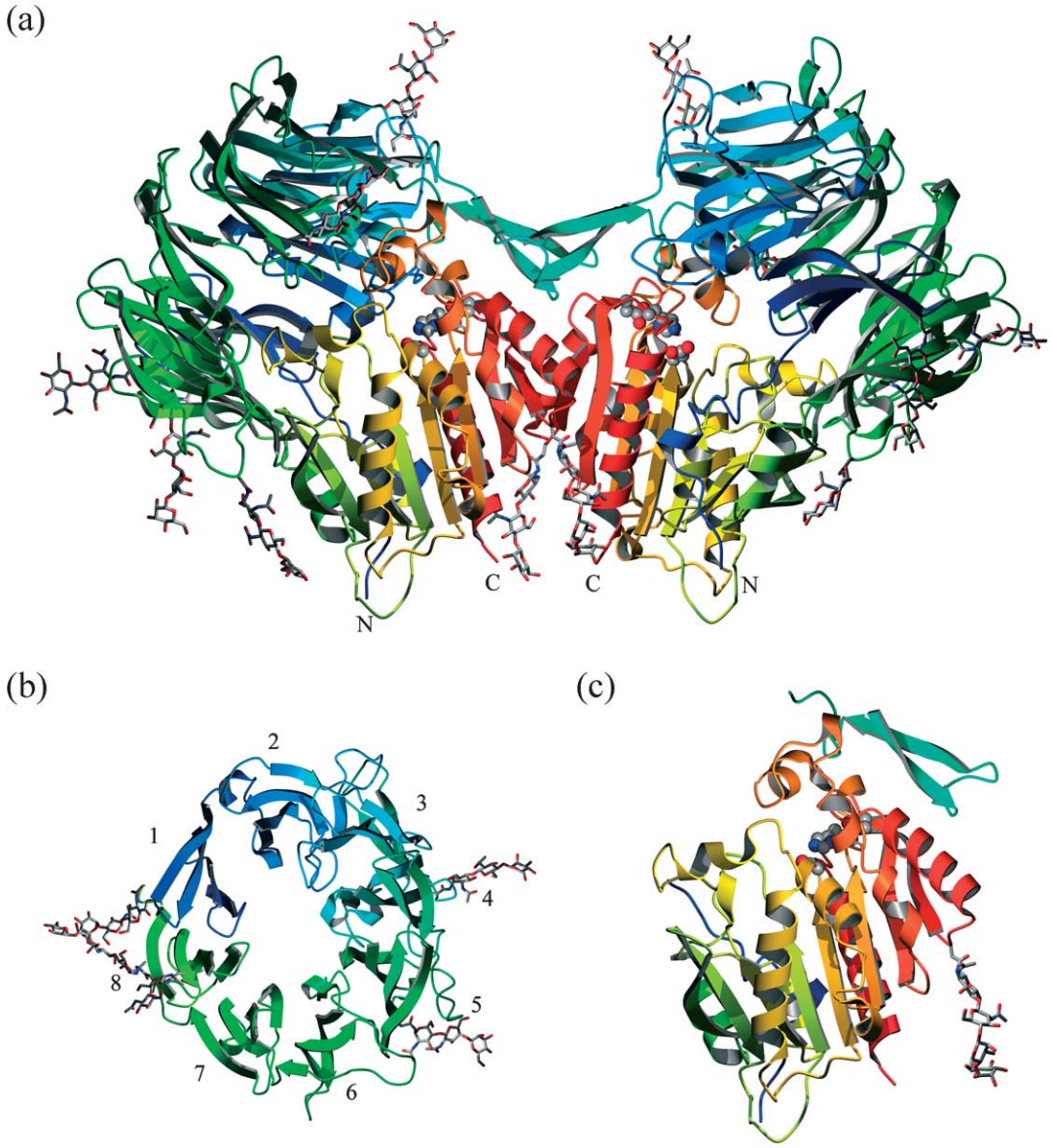


**Figure 1.** Structure of DPPX. (a) Ribbon diagram of the DPPX dimer. The color changes from blue (N terminus) to red (C terminus). Carbohydrates with glycosylation sites are shown in ball-and-stick representation and the "catalytic triad" is shown in CPK representation. (b) View of the eight-bladed β-propeller domain (residues 142–322, and 352–581). (c) View of the α/β hydrolase domain (residues 127–142, and 581–849). The color scheme is the same as used in (a). The Figure was created with POVSCRIPT[63,64] and POVRAY.

solution DPPX exists primarily as homodimers; however, small amounts of monomer, that over time self-associate to homodimers, were also observed (data not shown).

The asymmetric unit consists of two nearly identical dimers of DPPX. Residues 200–220 and some of the carbohydrates adopt different conformations in the four monomers and were excluded from non-crystallographic symmetry (NCS) restraints, which were applied to all atoms in the rest of the molecules. A superposition of the DPPX and DPP-IV structures is shown in Figure 2. The monomers of DPPX and DPP-IV superimpose with an r.m.s.d. value of 1.9 Å for 679 out of 722 α-carbon atoms, and 2.5 Å r.m.s.d. for the dimer.

## Active site

The active site of the dipeptidyl peptidases is located at the interface of the α/β domain and the β-propeller (Figure 1(a)). The tunnel through the β-propeller leading to the active site in DPPX is similar to the DPP-IV structure, where it is believed to allow for passage of substrate in and out of the active site. However, the DPPX "catalytic" triad (Asp712, Asp792, and His824) differs from the catalytic triad of active peptidases such as DPP-IV (Ser630, Asp708, His740) by substitution of the nucleophilic serine with aspartate (Figure 3(a) and b). Substitution of a larger side-chain for Ser630 causes a shift of 2.5 Å of His824 away from its

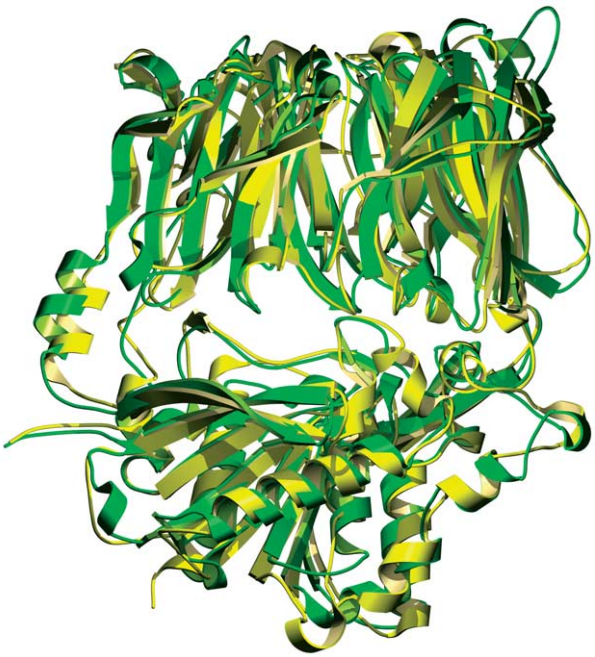

**Figure 2.** Ribbon diagram showing the superimposition of human DPPX (yellow), and human DPP-IV (green) monomers.

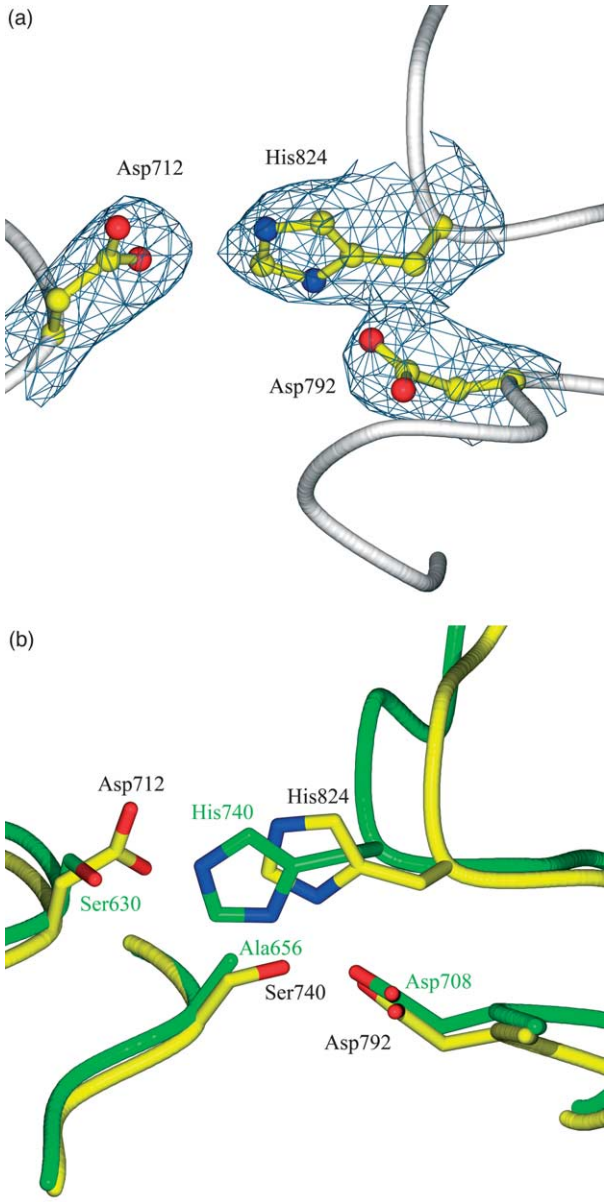


**Figure 3.** View of the active site environment of DPPX and DPP-IV. (a) $|F_o - F_c|$ $\sigma_A$-weighted omit map, calculated omitting the residues forming the "catalytic" triad, is contoured at 5σ (blue). (b) Diagram showing the superimposition of the active site of DPPX and DPP-IV. DPPX is shown in yellow, DPP-IV is in green. The catalytic triad of DPP-IV is formed by residues Ser630, Asp708, and His740. The analogous residues in DPPX are Asp712, Asp792, and His824. The additional serine residue (Ser740) in DPPX is alanine (Ala656) in the DPP-IV structure.

analogous position in the DPP-IV structure (Figure 3(b). Residues that are important for determination of dipeptidyl "amino" peptidase activity[29] (Glu205 and Glu206 in DPP-IV) are present in the DPPX structure in similar conformations as in the DPP-IV structure and could position the amino terminus in the active site in a similar fashion as in DPP-IV. However, the electrostatic sink (residues Arg125 and Asn710 in DPP-IV) that interacts with the carbonyl oxygen atom of the substrate in DPP-IV[29] has changed in the DPPX structure. Lys794 in DPPX (equivalent to Asn710 in DPP-IV) protrudes 2.5 Å further into the active site. Thus, a different substrate binding position might be necessary for substrate interaction with DPPX. Furthermore, DPPX has an additional serine residue (Ser740) in the vicinity of the active site, which is not present in DPP-IV (Ala565) (Figure 3(b)). In a typical serine protease, the catalytic serine transfers a proton to a nearby histidine, which is stabilized by the proximity of an aspartic acid. The geometry between Ser740, Asp792, and His824, however, is different from that found in active serine proteases. Although Asp792 still forms a hydrogen bond (2.7 Å) to His824, in DPPX Ser740 is not within hydrogen bonding distance of His824, and instead makes a hydrogen bond to Asp792 (3.0 Å). This arrangement of active site residues is inconsistent with the mechanism of serine proteases. Indeed, DPPX does not show any enzymatic activity to Gly-Pro-*p*-nitroanilide, which is used as an artificial substrate of DPP-IV.[13] DPPX also does not show any activity for several substrates of DPPI, DPPII and DPPIII[2] or in the QuantiCleave protease assay (Pierce; data not shown).

## Glycosylation

In contrast to nine glycosylation sites in the DPP-IV structure, there are seven predicted N-glycosylation sites for the DPPX sequence

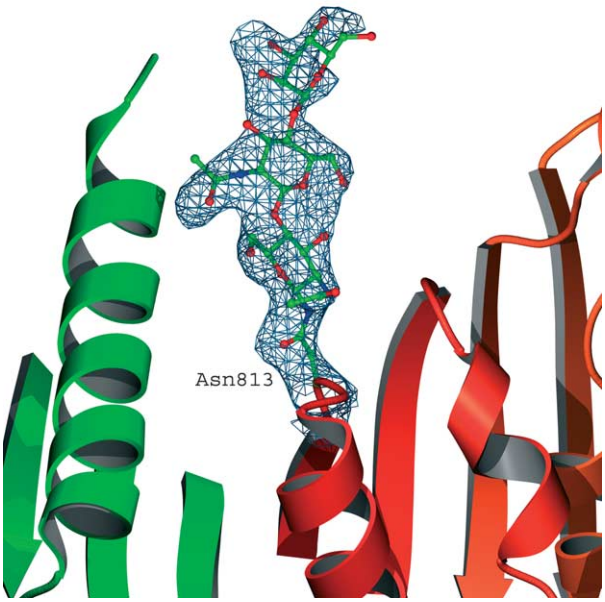


**Figure 4.** Simulated annealing $|2F_o-F_c|$ $\sigma_A$-weighed omit map, calculated omitting carbohydrate moieties at the dimer interface. DPPX is shown as a ribbon diagram, carbohydrates are shown in ball-and-stick representation. The omit map is contoured at 1σ (blue).

(Asn173, Asn319, Asn404, Asn471, Asn535, Asn566, and Asn813). We expressed DPPX in baculovirus-infected insect cells, which generally place high mannose carbohydrates of the form GCNac2Man3 at consensus asparagine residue-linked glycosylation sites. In the crystal structure of DPPX all seven sites, except for Asn471, have electron density consistent with at least two *N*-acetyl-glucosamine moieties, and in most sites electron density can be seen for one or two mannose moieties (Figure 1(a)). Most of the glycosylation sites occur in the β-propeller domain (blades 1,4, 6, and 8). The single glycosylation in the α/β hydrolase domain (Asn813) packs in a groove at the dimer interface (Figure 4). However, this glycosylation does not add any significant surface area to the dimer interface.

### Disulfides

There are four disulfide bridges in each monomer formed for cysteine pairs 411–418, 527–530, and 536–554 which are in blades 5,7, and 8, and for cysteine pair 735–846, which is in the α/β hydrolase domain near the C terminus of the molecule. Cys265 and Cys660 do not form disulfide bonds. Unlike the DPP-IV protein, DPPX does not have cysteine residues to form disulfide bonds in blade 6 of the β-propeller.

### Electrostatic surface

Calculations of the electrostatic potential yield vastly different results depending on the charge state of histidine (Figure 5). Inspection of the sequence of DPPX revealed a slightly higher abundance of histidine residues than in average proteins. On average, 2.1(±1.4)% of residues in protein sequences are histidines,[31] which does not change significantly based on protein localization in the cell.[31] Several dipeptidyl aminopeptidases have significantly higher than average histidine content (DPPX 3.3%; DPPY 3.5%; and DPP9 4.1%). Assuming a Gaussian distribution of histidine content among proteins, these values indicate that DPPX and DPPY have more histidine residues than 80–85% of all other extracellular proteins. This phenomenon, however, does not have a clear connection to their function at this point (Table 2). The net charge on the DPPX dimer changes from (−34 e) to (+16 e) upon histidine protonation (Figure 5(a) and (b)). A similar trend can be seen for DPP-IV; however, the overall charge on DPP-IV changes from more negative (−36 e) to nearly neutral (−2 e), rather then from negative to positive as seen for DPPX (Figure 5(c) and (d)). To determine the pI value of DPPX, isoelectric focusing (IEF) was performed. IEF results were comparable with the theoretical pI calculations and yielded a pI value of ∼5.8 (data not shown).

## Discussion

### Active site

Although the catalytic serine of dipeptidyl proteases is not present in DPPX, there is another serine residue in the vicinity of the active site (Ser740) (Figure 3(b)). A three-dimensional search with a query consisting of the coordinates of Ser740, His824, and Asp792 against known active sites in proteins[32] did not result in any positive matches. The relative geometry between Ser740, His824, and Asp792 is inconsistent with geometries of serine proteases, and appears not to be suited for catalysis. It is well known from a plethora of structure–function studies of serine proteases that the precise geometry of the catalytic triad is essential for catalytic activity. Thus, it is not surprising that the substantially altered structure of the region analogous to the DPP-IV active site is not catalytically active. The structure of the active site together with the failure of DPPX to cleave substrates of DPP-(I–IV) or cleave any sites within the limits of our assay suggest that DPPX has lost its peptidase function, and perhaps acquired a new function as a potassium channel accelerating factor. This phenomenon has been observed for other proteins such as DJ-1, which is 30% identical with a member of a cysteine protease family. The catalytic triad in DJ-1 has a permutated arrangement of catalytic residues and no proteolytic function has been detected.[33] However, DJ-1 was identified to have other functions including interactions with RNA binding proteins and an oxidative stress response. Association of Kv channels with auxiliary subunits that carry alternate function has also been reported.

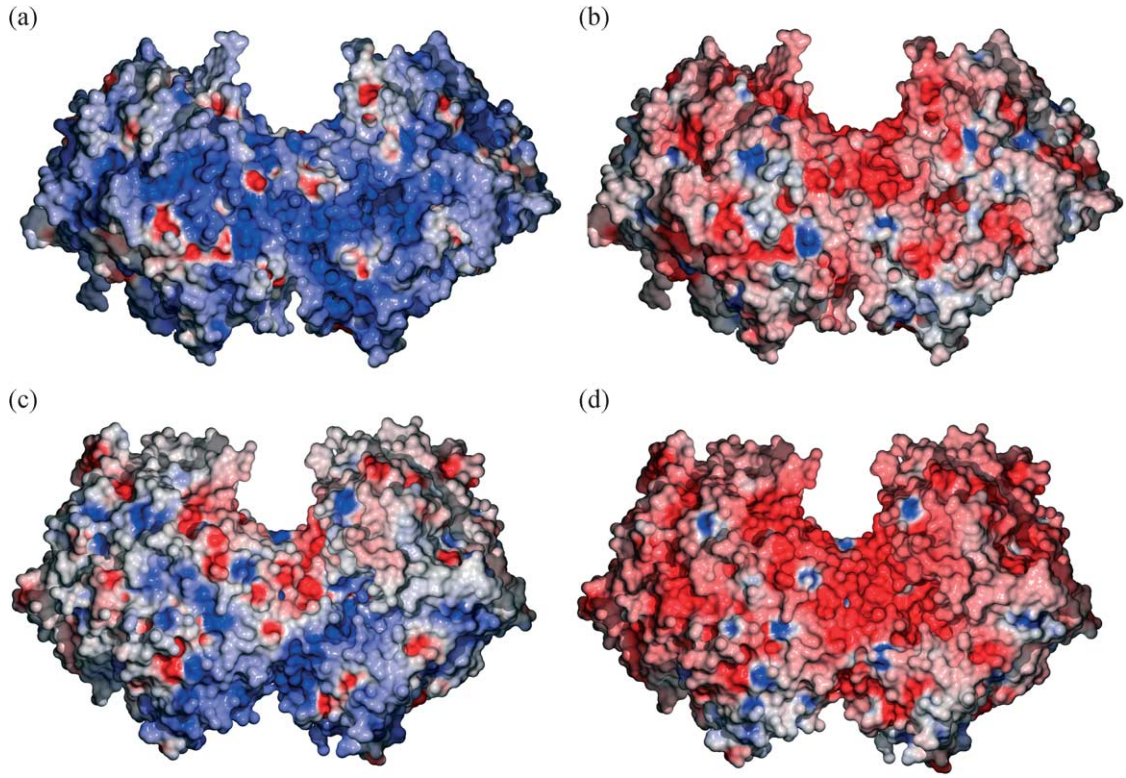


**Figure 5.** Molecular surfaces of DPPX and DPP-IV colored according to their electrostatic potential. ((a), (c)) The electrostatic potential for DPPX and DPP-IV, respectively, was calculated with a set of charges including a charged histidine residue. ((b), (d)) The electrostatic potential for DPPX and DPP-IV, respectively, was calculated with a charge set including de-protonated histidine residues. The details of the calculations are described in Materials and Methods. Potential values shown are in the range of $-15k_BT$ to $+15k_BT$ for all surfaces. The Figure was created with GRASP,[59] POVSCRIPT,[63] and POVRAY.

The Kvβ2 subunit, for example, is a member of an oxidoreductase family with a functional active site containing a nicotinamide cofactor.[34,35] Although the Kvβ2 subunit is a functional enzyme, it remains unclear if the enzymatic activity is coupled to channel function/regulation or if the oxidoreductase acts independently of its enzymatic function as a channel modulator.[36]

## Other possible functions of DPPX

Some dipeptidyl aminopeptidases have been reported to have multiple functions. In addition to its proteolytic function, DPP-IV functions as a binding partner for adenosine deaminase (ADA),[37] T-cell antigen (CD45),[37] and the $Na^+/H^+$ exchanger.[38] Given that some prolyl oligopeptidases have multiple functions, it is possible that DPPX, apart from associating with Kv4 pore-forming subunits, interacts with other proteins. DPPX contains β-propeller motifs that commonly act as scaffolds for protein–protein interactions.[4,39,40] In a report by the Prusiner laboratory,[41] DPPX was identified in a time-controlled transcardiac perfusion cross-linking study as one of the top candidates for interacting with the prion protein. In another report, DPPX was proposed to play a role in synaptic plasticity.[42] Disruption of gene encoding DPPX was also found to cause embryonic lethality in mice.[43] In contrast to DPP-IV, which is expressed in all organs,[11] DPPX and

**Table 2.** High abundance of histidine residues in the dipeptidyl aminopeptidase protein

| Family | His (%)[a] | His (#)[b] | +/−[c] | Theoretical pI | Net charge[d] per monomer |
|---|---|---|---|---|---|
| DPPX | 3.3 | 25 | 82/99 | 5.9 | −17/+8 |
| mDPPX | 3.5 | 26 | 85/100 | 6.0 | −15/+11 |
| hDPP10 | 3.5 | 26 | 77/92 | 6.0 | −15/+11 |
| hDPP9 | 4.1 | 35 | 86/105 | 6.0 | −19/+16 |
| hDPP8 | 3.3 | 28 | 90/116 | 5.6 | −26/+2 |
| hDPP-IV | 2.6 | 19 | 68/86 | 5.6 | −18/−1 |

[a] Histidine percentage in dipeptidyl aminopeptidases. In the average protein, 2.1(±1.4)% of residues are histidines.
[b] Total number of histidine residues in dipeptidyl aminopeptidase monomers.
[c] Number of positively (Arg and Lys) and negatively (Asp and Glu) charged residues in dipeptidyl aminopeptidase monomers.
[d] Net charge on dipeptidyl aminopeptidase monomers with a de-protonated and protonated histidine.

DPPY proteins are primarily expressed in the brain[1,3] (K. Takimoto, personal communication). More experiments will be necessary to determine whether DPPX, apart from being an important component of A-type $K^+$ channels, plays other roles such as mediating channel interactions with the extracellular matrix or binding to the prion protein.

### Kv4 interaction with DPPX

With our structure of DPPX, we can now speculate about its mode of interaction with the Kv4 channel. We attempted to utilize known structural information to rationalize the association of DPPX with Kv4, although very little functional data on this interaction exists. An electron density map at 21 Å resolution of a member of the Kv4 family (Kv4.2) complexed with KChIP2 was recently determined by single particle cryo-electron microscopy.[44] The structure shows that KChIP2 assembles with Kv4.2 subunits in a 4 : 4 stoichiometry and binds at the cytoplasmic side of the membrane to the tetramerization domain (T1) of Kv4.2. The binding site of KChIP at the Kv4.2 T1 domain does not overlap with that of Kvβ. Kvβ is also known to interact with the Kv4.2 α-subunit, although the ternary complex between Kv4.2, KChIP2, and Kvβ has not been observed.[44] A model is presented in Figure 6 based on the available structural and biochemical data.

The interaction between DPPX and Kv4.2 is poorly understood, and unlike the complex of Kv4.2 and KChIPs, residues that are responsible for DPPX binding to Kv4.2 are unknown. The cytoplasmic region of DPPX and DPPY proteins varies in length (31–95 amino acid residues) and is not homologous between the different DPPX isoforms and between DPPX and DPPY proteins. On the other hand, the region just before the transmembrane domain together with the transmembrane domain are homologous, making them good candidates for regions that interact with the Kv4 α-subunits. The N termini of the DPPX dimer point in the same direction and are located approximately 60 Å apart (Figure 6(e)). The dimension of the cross-section of the KvAP channel in the membrane is similar in size (50–80 Å). Structures of two voltage-sensitive channels MscS[45] and KvAP[46] reveal a loose packing of the voltage sensor helices against the remainder of the channel. The positions of the extracellular N termini of DPPX are consistent with the DPPX transmembrane domains either packing or interpolating near the periphery of the channel. Similar interactions have been proposed for the MinK (minimal $K^+$ channel subunit) related peptides (MiRPs).[47–49] MinK, as well as DPPX proteins might modulate the properties of channels by interpolation of transmembrane helices into the loosely packed periphery of the pore-forming subunits.[50,51]

### Stoichiometry of Kv4 and DPPX

The stoichiometry of interaction between pore-forming Kv4 α-subunits and DPPX has not yet been determined. Proteins that interact with Kv4 on the cytoplasmic side (KChIPs, and Kvβ) adopt a 4 : 4 stoichiometry. The same stoichiometry has also been seen for other potassium channels ($K_{ATP}$) associating with its auxiliary subunits.[52] DPPX exists primarily in a dimeric form, although a monomeric species has also been observed during purification. Monomeric DPPX, is not stable and over time self-associates and forms homodimers. No monomeric species were observed during purification of the mouse homolog of DPPX. In contrast to the soluble extracellular domain, the full length DPPX is embedded in the membrane and its orientation is governed by the transmembrane anchoring helix. This restraint could facilitate dimer formation and the full length DPPX may exist only as a dimer.

The formation of dipeptidyl aminopeptidase dimers can be somewhat promiscuous. DPPX and DPPY, like DPP-IV and FEP proteins, can form heterodimers[5] (K. Takimoto, personal communication). It appears that the formation of heterodimers is somewhat specific, as DPP-IV and DPPX cannot form heterodimers[5] (K. Takimoto, personal communication). The ability of DPPX to form heterodimers with DPPY but not with DPP-IV can arise from higher conservation of residues at the dimer interface. Residues at the dimer interface are 62% identical between DPPX and DPPY proteins, respectively, and 42% identical between DPPX and DPP-IV proteins, respectively. Also, the β-hairpin motif that forms a significant part of the dimer interface, differs between DPPX and DPP-IV structures. In the DPP-IV structure, there are additional three residues in this loop, resulting in an 8 Å pertrusion into the opposing monomer. Based on a sequence alignment and a homology model of DPPY, DPPY and DPPX have the same length of the β-hairpin motif. The longer β-hairpin loop of DPP-IV might interfere with formation of the DPP-IV/DPPX heterodimer. The functional implication of heterodimers is unclear at the moment.

Taken together it is likely that the interacting unit of DPPX is a dimer. Schematic representation of several possible organizations of DPPX dimers is shown in Figure 6(a)–(d). If the 4-fold symmetry of the channel is conserved (as seen for KChIPs and Kvβ2 interacting proteins) then either two or four dimers of DPPX would have to bind to Kv4. Given the large size of the extracellular domains of the DPPX dimer (200 kDa), it would be difficult to achieve packing of the transmembrane helices of four dimers of DPPX against the Kv4 channel and escape steric clashing in the extracellular space (Figure 6(c) and (d)). Thus, we speculate than either one dimer (2 : 4 stoichiometry), or a dimer of dimers (4 : 4 stoichiometry) of DPPX forms the DPPX:Kv4 complex (Figure 6(a) and (b)).

The recent electron microscopy structure of the complex of Kv4.2 and KChIP2 demonstrates that stable complexes of Kv4.2 can be purified and imaged. The large size of the DPPX protein will aid

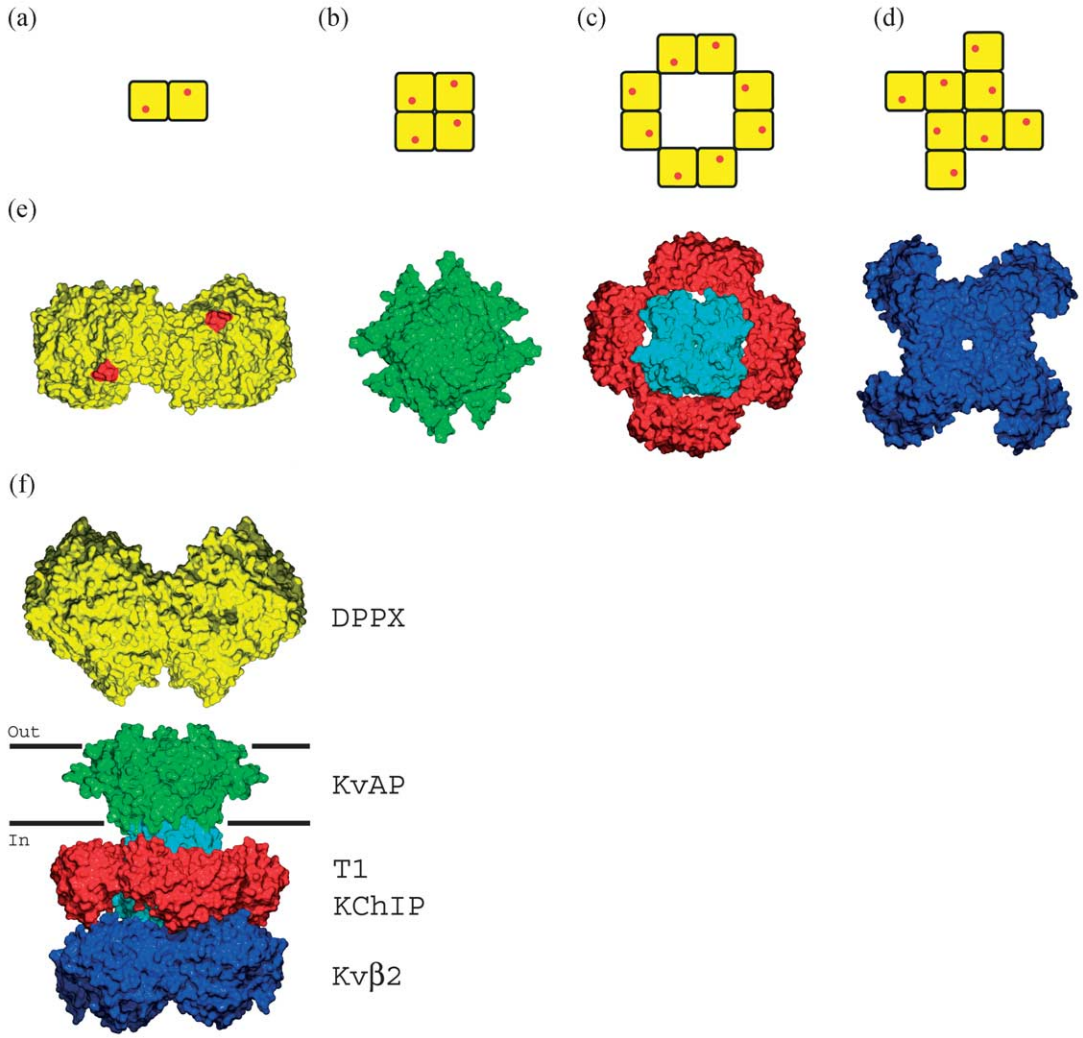


**Figure 6.** A theoretical model of proteins that might be involved in the formation of an A-type potassium channel complex ($I_{SA}$). Proteins are shown in surface representation and are all rendered on the same scale to show their relative sizes. ((a)–(d)) Schematic representation of several possible DPPX arrangements. Monomers that form the homodimer are colored yellow with the position of the transmembrane domains indicated by red dots. (e) The DPPX dimer is shown in yellow, KvAP (residues 22–80 and 145–240) is in green, four KChIP1s are in red, the T1 domain of Kv4.2 is in cyan, and Kvβ is in blue. Each N terminus of DPPX is colored in red, showing the approximate position where the DPPX transmembrane helix would connect. (f) Side view of the possible Kv4 channel super-complex. The approximate position of the membrane bilayer is indicated by black bars. Proteins are colored as for (e). It is unclear whether Kvβ can interact with the T1 domain of Kv4 at the same time as KChIP proteins.

in determination of the stoichiometry and geometry of binding to Kv4 channels. Although it is clear that more experiments will be necessary to understand the structure and function of A-type potassium channels in molecular detail, our structure of DPPX together with previously published data provide a good starting point for studying the Kv4 supermolecular complex.

## Materials and Methods

### Protein expression and purification

The extracellular domain of human DPPX (residues 117–865) was isolated by PCR from human brain cDNA library (Clontech) and cloned into the pAcGP67A vector (Pharmingen) in frame with the gp67 secretion sequence between XbaI and NotI restriction sites. For affinity purification, a His10 tag was added at the C terminus. *Spodoptera frugiperda* (Sf9) cells (Invitrogen) were transfected with pAcGP67A carrying the DPPX gene and linearized AcNPV DNA (Sapphire Baculovirus DNA; Orbigen) using Cellfectin (Invitrogen). Baculovirus was amplified in Sf9 cells in 10% (v/v) fetal bovine serum containing SF900-II medium (Gibco).

Large-scale protein expression was performed by infection of *Trichoplusia ni* (Hi5) cells in Insect-Xpress medium (Biowhitaker) at a cell density of $1.5\times10^6$ cells/ml with an infection course of 72 hours. The media containing the secreted, glycosylated, recombinant protein was concentrated and dialyzed using tangential flow filtration system (PALL) and subsequently "batch" purified with Ni-NTA resin (Qiagen) at 4 °C. Protein was eluted with 300 mM Imidazole (pH 7.5) and further purified by size-exclusion chromatography using a Superdex 200

16/60 column (Amersham Pharmacia Biotech) in buffer containing 50 mM Tris (pH 8.0), 150 mM NaCl, and 1 mM DTT. The peak corresponding to the DPPX dimer was then concentrated to 10 mg/ml in 100 kDa Centricon (Millipore) and used for crystallization trials.

### Crystallization, data collection and refinement

DPPX crystals were grown by the hanging drop method at 25 °C using a precipitant solution containing 100 mM Mes (pH 6.25), 22.5% (w/v) polyethylene glycol monomethyl ether 2000 (PEG MME 2000), 200 mM magnesium chloride, and 17.5% (v/v) glycerol. Thin plate-shaped crystals appeared in a few days, and grew to about 20 μm×100 μm×500 μm. Crystals were cross-linked with gluteraldehyde and then flash frozen in liquid nitrogen. Diffraction data were collected at Advanced Light Source (ALS) on beamline 8.2.1. The crystals belong to the space group $P2_1$ with unit cell dimensions $a$=69.0 Å, $b$=170.2 Å, $c$=159.3 Å, and β=92.1°. All data were processed with DENZO and SCALEPACK.[53]

The MODELLER server[54] was used to make a homology model of DPPX based on the known structure of DPP-IV,[12] which was then used for molecular replacement in the CCP4 program suite.[55] Two dimers were located in the asymmetric unit, and following rigid body refinement resulted in an *R*-factor of 50.0%. Alternate cycles of manual model building using the program O,[56] positional and individual *B*-factor refinement with the program CNS,[57] and addition of carbohydrates and water molecules to the model reduced the $R$ and $R_{free}$ values to 24.8% and 28.0%, respectively, for all of the reflections (3.0 Å resolution). During the refinement, NCS restraints of 300 kcal/mol Å$^2$ were applied in CNS to the four molecules in the asymmetric unit. Residues 200–220 and carbohydrates were excluded from the restraints, otherwise all remaining atoms were included. Release of the NCS restraints did not result in a drop of $R_{free}$ or significant changes to the structure and so they were kept at 300 kcal/mol Å$^2$ during the entire refinement process. Residues 471–475 and 725–729 in all monomers, and residues 209–213 in monomer D have weak electron density. A total of 72.5% of the residues in DPPX are in the most favored regions of the Ramachandran plot, 24.0% in the additional allowed regions as calculated with PROCHECK.[58] The final model contains 24,224 atoms (23,348 protein, 825 carbohydrate, and 51 water molecules).

### Protein Data Bank accession code

The coordinates for the structure have been deposited in the Protein Data Bank with accession number 1XFD.

### Electrostatic potential calculations

The electrostatic potential was calculated with program GRASP[59] with an interior dielectric of 2 and solvent dielectric of 80. The charge set used in the calculation was: (Lys Nζ +1 e, Arg Nη1 +0.5 e, Arg Nη2 +0.5 e, Glu Oε1 −0.5 e, Glu Oε2 −0.5 e, Asp Oδ1 −0.5 e, and Asp Oδ2 −0.5 e). For calculations using protonated histidine, His Nε2 +0.5 e, and His Nδ1 +0.5 e charges were used in addition to charges described above. The use of different program (APBS[60]) or charge sets (from force fields AMBER, CHARMM, and PARSE) produced the same results as with GRASP (data not shown). Potential values shown are in the range of $-15k_BT$ to $+15k_BT$ for all surfaces.

### Modeling of the Kv4.2 complex

The following structures were used in the model: DPPX, KvAP (pdb code 1ORQ),[46] Kv4.3 T1 domain (pdb code 1S1G),[61] KChiP1 (pdb code 1S6C),[62] and Kvβ-T1 domain complex (pdb code 1EXB).[35] The archeal homolog of Kv channels (KvAP) was used in the model. The mammalian channel would probably appear slightly taller and wider than shown in Figure 6. Residues 81–144 were omitted from the structure of KvAP, since the voltage sensor in the structure of KvAP is most likely not in its native conformation. Four KChip1 proteins were manually docked on the T1 domain (residues 38–145) based on the electron microscopy structure of the Kv4.2–KChIP2 complex[44] and based on the structure of the complex of the N terminus of Kv4.2 (residues 1–30) with KChIP1.[62] In the model, the N terminus of the T1 domain structure (residue 38) was placed in the proximity of the C terminus of the T1 domain (residues 1–30) bound to KChIP. Also, the hydrophobic surface of KchIP, which binds to the T1 domain, was oriented towards the T1 domain. For the Kvβ model, the Kvβ–T1 complex[35] was superimposed onto the structure of the T1 domain of Kv4.2. The assembly of the T1 domain, Kvβ, and KChip1 was then manually docked at the cytoplasmic side of the KvAP structure.

## Acknowledgements

We thank Erin J. Adams, Richard W. Aldrich, Marty J. Boulanger, Tim D. Fenn, Ezequiel H. Panepucci, Jon T. Sack, and Erdem Gultekin Tamguney for their technical assistance and for discussions. We also thank Koichi Takimoto for allowing us access to DPPY data prior to publication. This work is based upon research conducted at the Advanced Light Source, which is supported by the Director, Office of Science, Office of Energy Research, Office of Basic Energy Sciences, Materials Sciences Division, of the US Department of Energy under contract no. DE-AC03-76SF00098 at Lawrence Berkeley National Laboratory.

## References

1. Kin, Y., Misumi, Y. & Ikehara, Y. (2001). Biosynthesis and characterization of the brain-specific membrane protein DPPX, a dipeptidyl peptidase IV-related protein. *J. Biochem. (Tokyo)*, **129**, 289–295.
2. Wada, K., Yokotani, N., Hunter, C., Doi, K., Wenthold, R. J. & Shimasaki, S. (1992). Differential expression of two distinct forms of mRNA encoding members of a dipeptidyl aminopeptidase family. *Proc. Natl Acad. Sci. USA*, **89**, 197–201.
3. Nadal, M. S., Ozaita, A., Amarillo, Y., Vega-Saenz de Miera, E., Ma, Y., Mo, W. *et al*. (2003). The CD26-related dipeptidyl aminopeptidase-like protein DPPX is a critical component of neuronal A-type K+ channels. *Neuron*, **37**, 449–461.

4. Gorrell, M. D. (2003). First bite. *Nature Struct. Biol.* **10**, 3–5.
5. Scanlan, M. J., Raj, B. K., Calvo, B., Garin-Chesa, P., Sanz-Moncasi, M. P., Healey, J. H. *et al*. (1994). Molecular cloning of fibroblast activation protein alpha, a member of the serine protease family selectively expressed in stromal fibroblasts of epithelial cancers. *Proc. Natl Acad. Sci. USA*, **91**, 5657–5661.
6. Fulop, V., Bocskei, Z. & Polgar, L. (1998). Prolyl oligopeptidase: an unusual beta-propeller domain regulates proteolysis. *Cell*, **94**, 161–170.
7. Abbott, C. A., Yu, D. M., Woollatt, E., Sutherland, G. R., McCaughan, G. W. & Gorrell, M. D. (2000). Cloning, expression and chromosomal localization of a novel human dipeptidyl peptidase (DPP) IV homolog, DPP8. *Eur. J. Biochem.* **267**, 6140–6150.
8. Qi, S. Y., Riviere, P. J., Trojnar, J., Junien, J. L. & Akinsanya, K. O. (2003). Cloning and characterization of dipeptidyl peptidase 10, a new member of an emerging subgroup of serine proteases. *Biochem. J.* **373**, 179–189.
9. Rosenblum, J. S. & Kozarich, J. W. (2003). Prolyl peptidases: a serine protease subfamily with high potential for drug discovery. *Curr. Opin. Chem. Biol.* **7**, 496–504.
10. Polgar, L. (2002). The prolyl oligopeptidase family. *Cell Mol. Life Sci.* **59**, 349–362.
11. Mentlein, R. (1999). Dipeptidyl-peptidase IV (CD26)—role in the inactivation of regulatory peptides. *Regul. Pept.* **85**, 9–24.
12. Rasmussen, H. B., Branner, S., Wiberg, F. C. & Wagtmann, N. (2003). Crystal structure of human dipeptidyl peptidase IV/CD26 in complex with a substrate analog. *Nature Struct. Biol.* **10**, 19–25.
13. Yokotani, N., Doi, K., Wenthold, R. J. & Wada, K. (1993). Non-conservation of a catalytic residue in a dipeptidyl aminopeptidase IV-related protein encoded by a gene on human chromosome 7. *Hum. Mol. Genet.* **2**, 1037–1039.
14. Hille, B. (2001). *Ion Channels of Excitable Membranes* (3rd edit.). Sinauer Associates, Sunderland.
15. Herson, P. S. & Adelman, J. P. (2003). It takes two to tango, but three to ISA. *Neuron*, **37**, 370–372.
16. Jan, L. Y. & Jan, Y. N. (1997). Voltage-gated and inwardly rectifying potassium channels. *J. Physiol.* **505**, 267–282.
17. Song, W. J. (2002). Genes responsible for native depolarization-activated K+ currents in neurons. *Neurosci. Res.* **42**, 7–14.
18. Dixon, J. E., Shi, W., Wang, H. S., McDonald, C., Yu, H., Wymore, R. S. *et al*. (1996). Role of the Kv4.3 K+ channel in ventricular muscle. A molecular correlate for the transient outward current. *Circ. Res.* **79**, 659–668.
19. Tseng, G. N. (1999). Molecular structure of cardiac Ito channels: Kv4.2, Kv4.3, and other possibilities? *Cardiovasc. Res.* **41**, 16–18.
20. Amberg, G. C., Koh, S. D., Imaizumi, Y., Ohya, S. & Sanders, K. M. (2003). A-type potassium currents in smooth muscle. *Am. J. Physiol. Cell Physiol.* **284**, C583–C595.
21. Grace, A. A., Bunney, B. S., Moore, H. & Todd, C. L. (1997). Dopamine-cell depolarization block as a model for the therapeutic actions of antipsychotic drugs. *Trends Neurosci.* **20**, 31–37.
22. Liss, B., Franz, O., Sewing, S., Bruns, R., Neuhoff, H. & Roeper, J. (2001). Tuning pacemaker frequency of individual dopaminergic neurons by Kv4.3L and KChip3.1 transcription. *EMBO J.* **20**, 5715–5724.
23. Nadal, M. S., Amarillo, Y., Vega-Saenz de Miera, E. & Rudy, B. (2001). Evidence for the presence of a novel Kv4-mediated A-type K(+) channel-modifying factor. *J. Physiol.* **537**, 801–809.
24. Takimoto, K. & Ren, X. (2002). KChIPs (Kv channel-interacting proteins)—a few surprises and another. *J. Physiol.* **545**, 3.
25. An, W. F., Bowlby, M. R., Betty, M., Cao, J., Ling, H. P., Mendoza, G. *et al*. (2000). Modulation of A-type potassium channels by a family of calcium sensors. *Nature*, **403**, 553–556.
26. Kim, L. A., Furst, J., Butler, M. H., Xu, S., Grigorieff, N. & Goldstein, S. A. (2004). Ito channels are octomeric complexes with four subunits of each Kv4.2 and K+ channel-interacting protein 2. *J. Biol. Chem.* **279**, 5549–5554.
27. Jerng, H. H. & Pfaffinger, P. J. (2004). Biophysical Meeting Online Abstract, The Biophysical Society.
28. Oefner, C., D'Arcy, A., Mac Sweeney, A., Pierau, S., Gardiner, R. & Dale, G. E. (2003). High-resolution structure of human apo dipeptidyl peptidase IV/CD26 and its complex with 1-[([2-[(5-iodopyridin-2-yl) amino]-ethyl]amino)-acetyl]-2-cyano-(*S*)-pyrrol idine. *Acta Crystallog. D*, **59**, 1206–1212.
29. Engel, M., Hoffmann, T., Wagner, L., Wermann, M., Heiser, U., Kiefersauer, R. *et al*. (2003). The crystal structure of dipeptidyl peptidase IV (CD26) reveals its functional regulation and enzymatic mechanism. *Proc. Natl Acad. Sci. USA*, **100**, 5063–5068.
30. Aertgeerts, K., Ye, S., Tennant, M. G., Kraus, M. L., Rogers, J., Sang, B. C. *et al*. (2004). Crystal structure of human dipeptidyl peptidase IV in complex with a decapeptide reveals details on substrate specificity and tetrahedral intermediate formation. *Protein Sci.* **13**, 412–421.
31. Cedano, J., Aloy, P., Perez-Pons, J. A. & Querol, E. (1997). Relation between amino acid composition and cellular location of proteins. *J. Mol. Biol.* **266**, 594–600.
32. Stark, A. & Russell, R. B. (2003). Annotation in three dimensions. PINTS: Patterns in Non-homologous Tertiary Structures. *Nucl. Acids Res.* **31**, 3341–3344.
33. Wilson, M. A., Collins, J. L., Hod, Y., Ringe, D. & Petsko, G. A. (2003). The 1.1-Å resolution crystal structure of DJ-1, the protein mutated in autosomal recessive early onset Parkinson's disease. *Proc. Natl Acad. Sci. USA*, **100**, 9256–9261.
34. Gulbis, J. M., Mann, S. & MacKinnon, R. (1999). Structure of a voltage-dependent K+ channel beta subunit. *Cell*, **97**, 943–952.
35. Gulbis, J. M., Zhou, M., Mann, S. & MacKinnon, R. (2000). Structure of the cytoplasmic beta subunit-T1 assembly of voltage-dependent K+ channels. *Science*, **289**, 123–127.
36. Gulbis, J. M. (2002). The beta subunit of Kv1 channels: voltage-gated enzyme or safety switch? *Novartis Found. Symp.* **245**, 127–165.
37. Kameoka, J., Tanaka, T., Nojima, Y., Schlossman, S. F. & Morimoto, C. (1993). Direct association of adenosine deaminase with a T cell activation antigen, CD26. *Science*, **261**, 466–469.
38. Girardi, A. C., Degray, B. C., Nagy, T., Biemesderfer, D. & Aronson, P. S. (2001). Association of Na(+)–H(+) exchanger isoform NHE3 and dipeptidyl peptidase IV in the renal proximal tubule. *J. Biol. Chem.* **276**, 46671–46677.

39. Neer, E. J., Schmidt, C. J., Nambudripad, R. & Smith, T. F. (1994). The ancient regulatory-protein family of WD-repeat proteins. *Nature*, **371**, 297–300.
40. Yu, L., Gaitatzes, C., Neer, E. & Smith, T. F. (2000). Thirty-plus functional families from a single motif. *Protein Sci.* **9**, 2470–2476.
41. Schmitt-Ulms, G., Hansen, K. C., Liu, J., Cowdrey, C., Yang, J., DeArmond, S. J. *et al.* (2004). *In vivo* analysis of protein interactions involving the prion protein using time-controlled transcardiac perfusion cross-linking. *Nature Biotechnol.* **22**, 724–731.
42. de Lecea, L., Soriano, E., Criado, J. R., Steffensen, S. C., Henriksen, S. J. & Sutcliffe, J. G. (1994). Transcripts encoding a neural membrane CD26 peptidase-like protein are stimulated by synaptic activity. *Brain Res. Mol. Brain Res.* **25**, 286–296.
43. Hough, R. B., Lengeling, A., Bedian, V., Lo, C. & Bucan, M. (1998). Rump white inversion in the mouse disrupts dipeptidyl aminopeptidase-like protein 6 and causes dysregulation of Kit expression. *Proc. Natl Acad. Sci. USA*, **95**, 13800–13805.
44. Kim, L. A., Furst, J., Gutierrez, D., Butler, M. H., Xu, S., Goldstein, S. A. & Grigorieff, N. (2004). Three-dimensional structure of I(to); Kv4.2-KChIP2 ion channels by electron microscopy at 21 angstrom resolution. *Neuron*, **41**, 513–519.
45. Bass, R. B., Strop, P., Barclay, M. & Rees, D. C. (2002). Crystal structure of *Escherichia coli* MscS, a voltage-modulated and mechanosensitive channel. *Science*, **298**, 1582–1587.
46. Jiang, Y., Lee, A., Chen, J., Ruta, V., Cadene, M., Chait, B. T. & MacKinnon, R. (2003). X-ray structure of a voltage-dependent K+ channel. *Nature*, **423**, 33–41.
47. Melman, Y. F., Krummerman, A. & McDonald, T. V. (2002). KCNE regulation of KvLQT1 channels: structure–function correlates. *Trends Cardiovasc. Med.* **12**, 182–187.
48. Pourrier, M., Schram, G. & Nattel, S. (2003). Properties, expression and potential roles of cardiac K+ channel accessory subunits: MinK, MiRPs, KChIP, and KChAP. *J. Membr. Biol.* **194**, 141–152.
49. Abbott, G. W., Goldstein, S. A. & Sesti, F. (2001). Do all voltage-gated potassium channels use MiRPs? *Circ. Res.* **88**, 981–983.
50. Chen, H., Kim, L. A., Rajan, S., Xu, S. & Goldstein, S. A. (2003). Charybdotoxin binding in the I(Ks) pore demonstrates two MinK subunits in each channel complex. *Neuron*, **40**, 15–23.
51. Wang, W., Xia, J. & Kass, R. S. (1998). MinK–KvLQT1 fusion proteins, evidence for multiple stoichiometries of the assembled IsK channel. *J. Biol. Chem.* **273**, 34069–34074.
52. Zerangue, N., Schwappach, B., Jan, Y. N. & Jan, L. Y. (1999). A new ER trafficking signal regulates the subunit stoichiometry of plasma membrane K(ATP) channels. *Neuron*, **22**, 537–548.
53. Otwinowski, Z. & Minor, W. (1997). Processing of X-ray diffraction data collected in oscillation mode. *Methods Enzymol.* **276**, 307–326.
54. Fiser, A. & Sali, A. (2003). Modeller: generation and refinement of homology-based protein structure models. *Methods Enzymol.* **374**, 461–491.
55. Bailey, S. (1994). The CCP4 suite—programs for protein crystallography. *Acta Crystallog. D*, **50**, 760–763.
56. Jones, T. A., Zou, J. Y., Cowan, S. W. & Kjeldgaard, M. (1991). Improved methods for building protein models in electron-density maps and the location of errors in these models. *Acta Crystallog. A*, **47**, 110–119.
57. Brunger, A. T., Adams, P. D., Clore, G. M., DeLano, W. L., Gros, P., Grosse-Kunstleve, R. W. *et al.* (1998). Crystallography and NMR system: a new software suite for macromolecular structure determination. *Acta Crystallog. D*, **54**, 905–921.
58. Laskowski, R. A., Rullmannn, J. A., MacArthur, M. W., Kaptein, R. & Thornton, J. M. (1996). AQUA and PROCHECK-NMR: programs for checking the quality of protein structures solved by NMR. *J. Biomol. NMR*, **8**, 477–486.
59. Nicholls, A. & Honig, B. (1992). *GRASP: Graphical Representation and Analysis of Surface Properties*. Columbia University, New York.
60. Baker, N. A., Sept, D., Joseph, S., Holst, M. J. & McCammon, J. A. (2001). Electrostatics of nanosystems: application to microtubules and the ribosome. *Proc. Natl Acad. Sci. USA*, **98**, 10037–10041.
61. Scannevin, R. H., Wang, K., Jow, F., Megules, J., Kopsco, D. C., Edris, W. *et al.* (2004). Two N-terminal domains of Kv4 K(+) channels regulate binding to and modulation by KChIP1. *Neuron*, **41**, 587–598.
62. Zhou, W., Qian, Y., Kunjilwar, K., Pfaffinger, P. J. & Choe, S. (2004). Structural insights into the functional interaction of KChIP1 with Shal-type K(+) channels. *Neuron*, **41**, 573–586.
63. Fenn, T. D., Ringe, D. & Petsko, G. A. (2003). POVScript+ program for model and data visualization using persistence of vision ray tracing. *J. Appl. Crystallog.* **36**, 944–947.
64. Kraulis, P. J. (1991). MOLSCRIPT: a program to produce both detailed and schematic plots of protein structures. *J. Appl. Crystallog.* **24**, 946–950.


***Edited by R. Huber***

*(Received 16 June 2004; received in revised form 20 August 2004; accepted 2 September 2004)*